CD72 negatively regulates B lymphocyte responses to the lupus–related endogenous toll–like receptor 7 ligand Sm/RNP

Chizuru Akatsu,[1]* Kenro Shinagawa,[2]* Nobutaka Numoto,[2]* Zhihong Liu,[1,3] Ayse Konuskan Ucar,[1] Mohammad Aslam,[1] Shirly Phoon,[1] Takahiro Adachi,[1] Koji Furukawa,[4] Nobutoshi Ito,[2] and Takeshi Tsubata[1]

[1]Department of Immunology and [2]Department of Structural Biology, Medical Research Institute, Tokyo Medical and Dental University, Bunkyo, Tokyo 113-8510, Japan
[3]Emergency Department, The First Affiliated Hospital of China Medical University, Shenyang, Liaoning Province 110001, China
[4]Biomedical Research Institute, National Institute of Advanced Industrial Science and Technology, Tsukuba, Ibaraki 305-8566, Japan

Toll–like receptor 7 (TLR7) plays an essential role in development of systemic lupus erythematosus by co–stimulating B cells reactive to the endogenous TLR7 ligand Sm/ribonucleoprotein (RNP), a crucial lupus self–antigen. However, how the TLR7–mediated autoimmune response is regulated is not yet known. In this study, we demonstrate that CD72, an inhibitory B cell co–receptor known to prevent development of lupus, recognizes Sm/RNP at the extracellular C–type lectin–like domain (CTLD) and specifically inhibits B cell response to Sm/RNP. Moreover, the CTLD of *CD72*[c], a lupus–susceptible allele, binds to Sm/RNP less strongly than that of lupus–resistant *CD72*[a]. Reduced binding of CD72[c] is supported by x–ray crystallographic analysis that reveals a considerable alteration in charge at the putative ligand–binding site. Thus, CD72 appears to specifically inhibit B cell response to the endogenous TLR7 ligand Sm/RNP through CTLD–mediated recognition of Sm/RNP, thereby preventing production of anti–Sm/RNP antibody crucial for development of lupus.

INTRODUCTION

CD72, a type II membrane protein expressed mostly in B cells, contains a C-type lectin-like domain (CTLD) in the extracellular region and an immunoreceptor tyrosine–based inhibition motif (ITIM) in the cytoplasmic region (Nitschke and Tsubata, 2004; Tsubata, 2012). By recruiting SH2 domain–containing phosphatase 1 (SHP-1) to the phosphorylated ITIM, CD72 negatively regulates B cell antigen receptor (BCR) signaling.

Several lines of evidence suggest that CD72 plays a role in regulation of the development of systemic lupus erythematosus (SLE), a prototype systemic autoimmune disease characterized by production of autoantibodies to various nuclear components and inflammatory lesions caused by deposition of immune complexes. First, polymorphism of *CD72* associates with lupus in both human and mice (Qu et al., 2000; Hitomi et al., 2004). There are three characterized mouse *CD72* alleles, i.e., *CD72*[a], *CD72*[b], and *CD72*[c]

(Tung et al., 1986; Robinson et al., 1992; Ying et al., 1995). CD72[a] and CD72[b] are highly conserved. In contrast, the extracellular region of CD72[c] has a marked difference from the other alleles including several amino acid substitutions and a seven–amino acid deletion in CTLD, although the amino acid sequence of the transmembrane and cytoplasmic regions of CD72[c] is identical to that of the other alleles. *CD72*[c] is associated with lupus-like disease in MRL.*Fas*[lpr/lpr] mice (Qu et al., 2000), and replacement of *CD72*[c] by *CD72*[b] reduces the severity of the autoimmune disease (Oishi et al., 2013; Xu et al., 2013). Second, *CD72*^{−/−} mice spontaneously develop lupus-like disease when they age (Li et al., 2008), and development of the disease is accelerated by *Fas*[lpr] (Xu et al., 2013). Remarkably, *CD72*^{−/−} *Fas*[lpr/lpr] mice on the C57BL/6 background develop severe autoimmune disease comparable with that in MRL.*Fas*[lpr/lpr] mice (Xu et al., 2013), whereas C57BL/6 mice carrying *Fas*[lpr/lpr] do not develop autoimmune disease (Izui et al., 1984).

Although overexpression of CD72 negatively regulates BCR signaling in B cell lines (Adachi et al., 2000), studies with primary B cells from *CD72*^{−/−} mice showed that CD72 only marginally regulates BCR signaling induced by BCR ligation using anti-IgM antibody (Xu et al.,
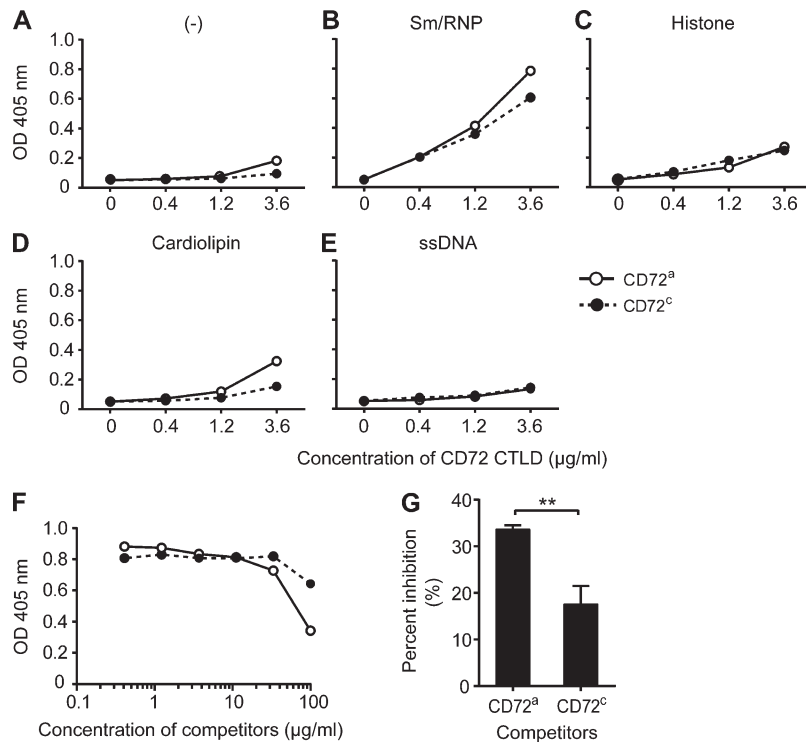
Figure 1. **CD72 CTLD specifically binds to Sm/RNP.** (A–E) Conventional ELISA. Biotinylated CD72[a] and CD72[c] CTLD proteins at the indicated concentrations were incubated with ELISA plates coated with the indicated molecules. CD72 CTLD proteins bound to the ELISA plates were detected using alkaline phosphatase–conjugated streptavidin and phosphatase substrate. Data are representative of five independent experiments. (F and G) Competitive ELISA. (F) Binding of biotinylated CD72[c] CTLD to Sm/RNP in the presence of various concentrations of unbiotinylated CD72[a] and CD72[c] CTLD proteins was measured. Representative data of five independent experiments are shown. (G) Mean ± SD of percent inhibition of binding in the presence of 100 µg/ml of the indicated competitors in triplicate is shown. **, $P < 0.01$ (two-tailed Student's t test).

2013). In contrast, BCR signaling is strongly regulated by other ITIM-containing inhibitory receptors such as CD22 and PIR-B (Otipoby et al., 1996; Sato et al., 1996; Nitschke et al., 1997; Ujike et al., 2002). Nonetheless, deficiency in CD22 or PIR-B alone does not cause autoimmune disease (Jellusova et al., 2010; Takai et al., 2011), and development of autoimmune disease requires an additional defect in Siglec-G or Fas, respectively (Kubo et al., 2009; Jellusova et al., 2010). To address the conflicting findings that CD72 does not regulate polyclonal BCR signaling induced by anti-IgM antibody but strongly inhibits development of lupus-like disease, we hypothesized that CD72 recognizes lupus-related self-antigens and specifically regulates self-reactive B cells without influencing overall BCR signaling of polyclonal B cells. Here, we demonstrate that the CTLD of CD72 binds to the Sm/ribonucleoprotein (RNP) antigen, a lupus-related RNA-containing nuclear self-antigen (Tan, 1989) and an endogenous TLR7 ligand (Lau et al., 2005), and CD72 specifically regulates B cell response to Sm/RNP but not a synthetic TLR7 ligand. Moreover, x-ray crystallographic analysis showed marked alteration of the putative ligand-binding site in CD72[c] compared with CD72[a], which appears to be involved in reduced binding affinity of CD72[c] to Sm/RNP. Because autoimmune B cell response to Sm/RNP plays a crucial role in lupus (James et al., 1995; Berland et al., 2006; Christensen et al., 2006), our results strongly suggest that CD72 regulates development of lupus by recognizing Sm/RNP and that *CD72[c]* functions as an SLE susceptibility gene because of poor binding to Sm/RNP.

RESULTS
CD72 CTLD binds to Sm/RNP
To address whether CD72 recognizes lupus-related self-antigens, we constructed the expression plasmids encoding CD72[a] CTLD or that of CD72[c] CTLD together with the His-tag and Avi-tag, a peptide allowing biotinylation by the enzyme BirA (Schatz, 1993; Beckett et al., 1999). By introducing these vectors into BirA-expressing bacteria, we prepared biotinylated CD72[a] CTLD and CD72[c] CTLD proteins. When we examined binding of these proteins to lupus-related self-antigens DNA, histone, Sm/RNP, and cardiolipin by ELISA, both CD72[a] CTLD and CD72[c] CTLD bound to Sm/RNP but not other self-antigens (Fig. 1, A–E). As CD72[a] CTLD binds to Sm/RNP modestly better than CD72[c] CTLD, we prepared CD72[a] CTLD and CD72[c] CTLD proteins without tag and compared binding of these proteins to Sm/RNP by competitive ELISA. CD72[a] CTLD inhibited the binding of biotinylated CD72 to Sm/RNP more efficiently than CD72[c] CTLD (Fig. 1, F and G), suggesting that CD72[a] CTLD binds to Sm/RNP more strongly than CD72[c] CTLD.

Next, we confirmed binding of CD72 CTLD to Sm/RNP by surface plasmon resonance (SPR) analysis. We prepared CD72[a] CTLD and CD72[c] CTLD proteins without tag, immobilized these proteins, and then injected various concentrations of Sm/RNP. Both CD72[a] CTLD and CD72[c] CTLD bound to Sm/RNP in a dose-dependent manner (Fig. 2, A and B). The dissociation constant of CD72[a] CTLD was lower than that of CD72[c] CTLD (Fig. 2 C), suggesting that CD72[a] binds to Sm/RNP with higher affinity than CD72[c]. Collectively, CD72 specifi-
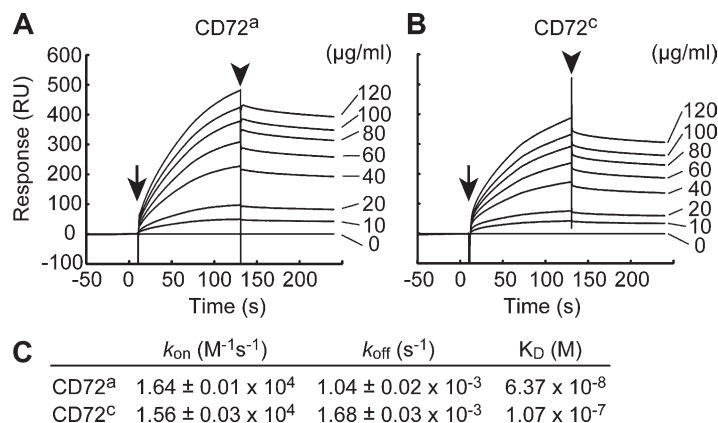
A CD72[a]

B CD72[c]

C

	k_{on} (M^{-1}s^{-1})	k_{off} (s^{-1})	K_D (M)
CD72[a]	$1.64 \pm 0.01 \times 10^4$	$1.04 \pm 0.02 \times 10^{-3}$	6.37×10^{-8}
CD72[c]	$1.56 \pm 0.03 \times 10^4$	$1.68 \pm 0.03 \times 10^{-3}$	1.07×10^{-7}

Figure 2. **SPR analysis of the binding of CD72[a] CTLD and CD72[c] CTLD to Sm/RNP.** (A and B) SPR sensorgrams representing binding of Sm/RNP to immobilized recombinant CD72[a] CTLDc/s (A) and CD72[c] CTLDc/s (B) proteins. The indicated concentrations of Sm/RNP were injected over the sensor chip. Arrows and arrowheads indicate the beginning of association and dissociation phases, respectively. RU, resonance units. (C) The kinetic parameter association rate constant (k_{on}) and dissociation rate constant (k_{off}) were determined by BIAevaluation software. K_D values were calculated from k_{on} and k_{off} values. A molecular weight of Sm/RNP was assumed to be 250 kD to calculate the kinetic parameters. Data are representative of two independent experiments.

cally binds to Sm/RNP, and binding affinity of CD72[a] is higher than that of CD72[c].

X–ray crystallographic analysis of CD72[a] CTLD and modeling of CD72[c] CTLD

To obtain structural insight of the function of CD72 CTLD, we determined the crystal structure of CD72[a] CTLD in a ligand-free form at 1.2 Å resolution. The overall structure of CD72[a] CTLD (Fig. 3 A) is very similar to that of the typical CTLD fold (Zelensky and Gready, 2005), which is composed of two α helices, two antiparallel β sheets, and three disulfide bonds. However, the amino acid sequence between the α2 helix and the β3 strand is shorter than those of other CTLDs (Fig. 3, B–G). Although this region contains various secondary structures such as β strands and a Ca^{2+}-binding site in some CTLDs (Feinberg et al., 2001; Swaminathan et al., 2005), CD72[a] CTLD contains only a distorted β strand and a short loop connecting the α2 helix and the β3 strand without a Ca^{2+}-binding site. In addition, an insertion at the L1 loop region is observed in both mouse and human CD72 CTLDs. Interestingly, the insertion contains a unique cluster of aromatic residues consisting of Tyr276, Tyr277 (Phe277 in CD72[c]), and Tyr278 (Fig. 3 G) in mouse CD72 and Tyr281, Tyr282, and Phe283 in human CD72.

Analysis of the electrostatic potentials of CD72[a] CTLD reveals that there is a highly positively charged patch on the surface in the region containing the β3 and β4 strands of CD72[a] CTLD (Fig. 4 A). The β3 and β4 strands are involved in ligand binding in other CTLDs such as eosinophil major basic protein (EMBP) and dendritic cell–specific intracellular adhesion molecule 3–grabbing nonintegrin (DC-SIGN; Feinberg et al., 2001; Swaminathan et al., 2005). Indeed, EMBP contains a positively charged patch similar to that of CD72[a] CTLD in the corresponding region involved in binding to sulfated glycosides with negatively charged sulfate ions (Swaminathan et al., 2005), whereas the negatively charged corresponding region of DC-SIGN interacts with Ca^{2+} required for ligand binding (Fig. 4 B; Feinberg et al., 2001). Thus, the positively charged patch found in CD72[a] CTLD appears to be a part of its ligand-binding site that binds to

ligands with a strong negative charge such as nucleic acid and may be involved in recognition of Sm/RNP that contains the small nuclear RNA.

To address the structure of CD72[c] CTLD, we first analyzed distribution of amino acids in CD72[a] CTLD that are different from CD72[c] CTLD (Fig. 4 C). All the amino acids in CD72[a] CTLD that are substituted by different ones in CD72[c] CTLD are located in the molecular surface (Fig. 4 D), and both amino acids in the hydrophobic core region and all the six cysteine residues forming the three intermolecular disulfide bonds are conserved between CD72[a] and CD72[c]. This strongly suggests that CD72[c] CTLD forms an overall structure very similar to that of CD72[a] CTLD. Because of this overall structural similarity between CD72[a] and CD72[c] CTLD, we generated the homology model of CD72[c] CTLD based on the x-ray crystal structure of CD72[a] CTLD, as we were unable to obtain good crystals of CD72[c] CTLD. The model shows a very different charge distribution in the putative ligand-binding region compared with CD72[a] CTLD (Fig. 4 A); substitutions of the basic residues of CD72[a] CTLD located in the β3 and β4 strands (Fig. 4 C) result in generation of a negative-charge patch. To experimentally address the distinct surface charge of CD72[c] CTLD, we examined the binding properties to a cation exchange column (Fig. 4 E) and found that CD72[a] CTLD tightly binds to the column, whereas CD72[c] CTLD does not bind to the same column. This result clearly demonstrates that the surface of CD72[c] CTLD is not so much positively charged as CD72[a] CTLD and, thus, supports the presence of a negatively charged patch in the homology model of CD72[c] CTLD.

CD72 specifically regulates B cell responses to Sm/RNP

As CD72 binds to Sm/RNP, we addressed whether CD72 specifically regulates B cell responses to Sm/RNP. We conjugated 4-hydroxy-3-nitrophenyl acetyl (NP) to BSA and Sm/RNP (NP-BSA and NP-Sm/RNP, respectively) and ligated BCR with these antigens in B cells from *CD72^{+/+}* and *CD72^{-/-}* quasimonoclonal (QM) mice. Because most of the B cells in QM mice are reactive to NP (Cascalho et al., 1996), treatment of QM B cells with NP-Sm/RNP and NP-BSA
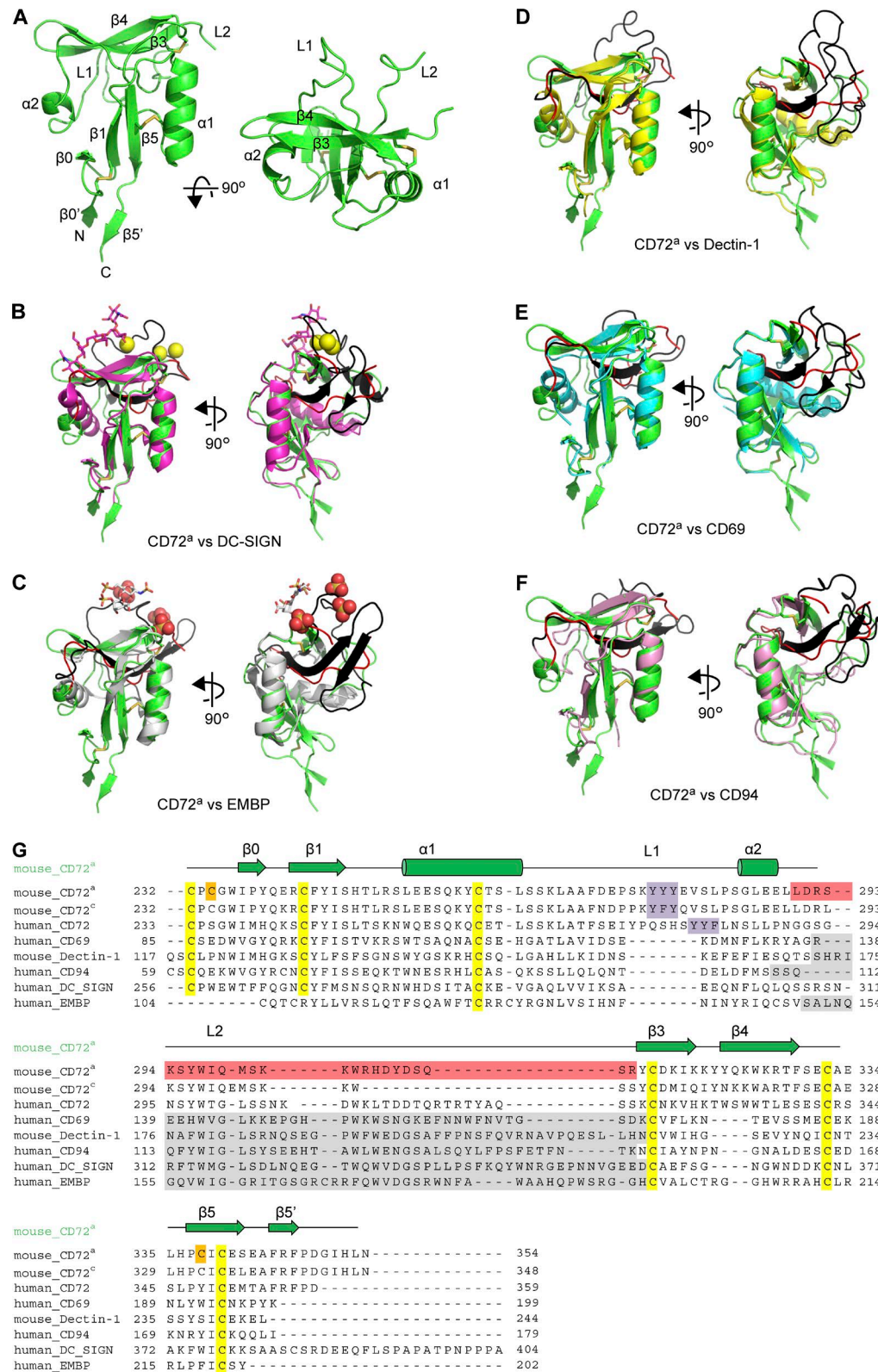
G

mouse_CD72ᵃ

mouse_CD72ᵃ	232	--CPCGWIPYQERCFYISHTLRSLEESQKYCTS-LSSKLAAFDEPSKYYYEVSLPSGLEELLDRS--	293
mouse_CD72ᶜ	232	--CPCGWIPYQKRCFYISHTLRSLEESQKYCTS-LSSKLAAFNDPPKYFYQVSLPSGLEELLDRL--	293
human_CD72	233	--CPSGWIMHQKSCFYISLTSKNWQESQKQCET-LSSKLATFSEIYPQSHSYYFLNSLLPNGGSG--	294
human_CD69	85	---CSEDWVGYQRKCYFISTVKRSWTSAQNACSE-HGATLAVIDSE-------KDMNFLKRYAGR--	138
mouse_Dectin-1	117	QSCLPNWIMHGKSCYLFSFSGNSWYGSKRHCSQ-LGAHLLKIDNS-------KEFEFIESQTSSHRI	175
human_CD94	59	CSCQEKWVGYRCNCYFISSEQKTWNESRHLCAS-QKSSLLQLQNT-------DELDFMSSSQ-----	112
human_DC_SIGN	256	--CPWEWTFFQGNCYFMSNSQRNWHDSITACKE-VGAQLVVIKSA-------EEQNFLQLQSSRSN-	311
human_EMBP	104	---------CQTCRYLLVRSLQTFSQAWFTCRRCYRGNLVSIHNF-------NINYRIQCSVSALNQ	154

mouse_CD72ᵃ

mouse_CD72ᵃ	294	KSYWIQ-MSK------KWRHDYDSQ--------------SRYCDKIKKYYQKWKRTFSECAE	334
mouse_CD72ᶜ	294	KSYWIQEMSK------KW----------------------SSYCDMIQIYNKKWARTFSECAE	328
human_CD72	295	NSYWTG-LSSNK----DWKLTDDTQRTRTYAQ----------SSKCNKVHKTWSWWTLESESCRS	344
human_CD69	139	EEHWVG-LKKEPGH---PWKWSNGKEFNNWFNVTG--------SDKCVFLKN----TEVSSMECEK	188
mouse_Dectin-1	176	NAFWIG-LSRNQSEG--PWFWEDGSAFFPNSFQVRNAVPQESL-LHNCVWIHG----SEVYNQICNT	234
human_CD94	113	QFYWIG-LSYSEEHT--AWLWENGSALSQYLFPSFETFN-----TKNCIAYNPN---GNALDESCED	168
human_DC_SIGN	312	RFTWMG-LSDLNQEG--TWQWVDGSPLLPSFKQYWNRGEPNNVGEEDCAEFSG----NGWNDDKCNL	371
human_EMBP	155	GQVWIG-GRITGSGRCRRFQWVDGSRWNFA----WAAHQPWSRG-GHCVALCTRG--GHWRRAHCLR	214

mouse_CD72ᵃ

mouse_CD72ᵃ	335	LHPCICESEAFRFPDGIHLN-------------	354
mouse_CD72ᶜ	329	LHPCICELEAFRFPDGIHLN-------------	348
human_CD72	345	SLPYICEMTAFRFPD------------------	359
human_CD69	189	NLYWICNKPYK----------------------	199
mouse_Dectin-1	235	SSYSICEKEL-----------------------	244
human_CD94	169	KNRYICKQQLI----------------------	179
human_DC_SIGN	372	AKFWICKKSAASCSRDEEQFLSPAPATPNPPPA	404
human_EMBP	215	RLPFICSY-----------------------	202

Figure 3. **Structure of CD72ᵃ CTLD and comparisons to other CTLDs.** (A) Overall structure of CD72ᵃ CTLD represented as a ribbon diagram. Disulfide bonds are shown as a stick model. Secondary structures are indicated. Representative data of five independent experiments are shown. (B–F) Ribbon models of CTLDs of DC-SIGN (B), EMBP (C), dectin-1 (D), CD69 (E), and CD94 (F) are represented as magenta, gray, yellow, cyan, and pink, respectively, and

mimics interaction of anti-Sm/RNP and anti-BSA B cells with corresponding antigens, respectively (Fig. 5 A). When we stimulated $CD72^{+/+}$ and $CD72^{-/-}$ QM B cells with NP-Sm/RNP, Ca^{2+} mobilization was augmented in $CD72^{-/-}$ QM B cells compared with $CD72^{+/+}$ QM B cells (Fig. 5 B). In contrast, the level of Ca^{2+} mobilization induced by NP-BSA in $CD72^{-/-}$ QM B cells was similar to that in $CD72^{+/+}$ QM B cells. This result suggested that CD72 specifically regulates BCR signaling induced by Sm/RNP.

We next addressed B cell proliferation by CFSE dilution assay. B cell proliferation induced by anti-IgM antibody in $CD72^{-/-}$ QM B cells was similar to that in $CD72^{+/+}$ QM B cells (Fig. 5, C and D), in agreement with our previous finding that anti-IgM–induced Ca^{2+} mobilization and B cell proliferation were not different between $CD72^{+/+}$ and $CD72^{-/-}$ B cells (Xu et al., 2013). Treatment with NP-BSA and NP-Sm/RNP did not induce proliferation of $CD72^{+/+}$ QM B cells. In contrast, NP-Sm/RNP but not NP-BSA induced proliferation of $CD72^{-/-}$ QM B cells (Fig. 5, C and D). This result clearly demonstrated that CD72 regulates B cell response to Sm/RNA but not BSA or anti-IgM. As Sm/RNP is a TLR7 agonist (Lau et al., 2005), we addressed whether CD72 regulates other TLR7 ligands. When we treated $CD72^{+/+}$ and $CD72^{-/-}$ B cells with the synthetic TLR7 agonist imiquimod (Hemmi et al., 2002), proliferation of $CD72^{-/-}$ B cells was comparable with that of $CD72^{+/+}$ B cells (Fig. 5, E and F), suggesting that CD72 regulates B cell activation induced by Sm/RNP but not other TLR7 agonists. Thus, CD72 specifically inhibits B cell response to the endogenous TLR7 agonist Sm/RNP.

As BCR endocytosis depends on BCR ligation–induced activation of signaling molecules such as Rac (Phee et al., 2001; Malhotra et al., 2009), we addressed whether CD72 regulates BCR endocytosis. We incubated $CD72^{+/+}$ and $CD72^{-/-}$ QM B cells with NP-BSA or NP-Sm/RNP on ice so that BCRs on the surface were occupied by the antigens. After washing, we incubated these B cells at 37°C and measured the amount of remaining antigens on the cell surface by flow cytometry. When BCR was ligated by NP-BSA, the amount of NP-BSA on the cell surface was reduced in $CD72^{-/-}$ QM B cells at the same rate as in $CD72^{+/+}$ QM B cells (Fig. 6, A and B). In contrast, reduction of NP-Sm/RNP was faster in $CD72^{-/-}$ B cells than that in $CD72^{+/+}$ B cells (Fig. 6, C and D). This result clearly demonstrated that CD72 regulates BCR-mediated endocytosis of NP-Sm/RNP but

not NP-BSA. Collectively, CD72 specifically down-regulated BCR signaling, B cell proliferation, and BCR-mediated endocytosis induced by Sm/RNP.

Coligation of CD72 and BCR is required for signal inhibition

CD72 inhibits BCR signaling by recruiting SHP-1 to its phosphorylated ITIM (Nitschke and Tsubata, 2004; Tsubata, 2012). To address how CD72 specifically regulates B cell response to Sm/RNP, we treated the B cell line BAL17-9T13 that expresses anti-NP BCR of IgM class with NP-Sm/RNP or NP-BSA. CD72 was strongly phosphorylated and recruited SHP-1 upon stimulation with NP-Sm/RNP, whereas treatment with NP-BSA alone failed to enhance phosphorylation or SHP-1 recruitment of CD72 (Fig. 7, A–D). Moreover, simultaneous treatment with Sm/RNP and NP-BSA did not enhance phosphorylation or SHP-1 recruitment of CD72, indicating that independent ligation of BCR and CD72 does not induce signal inhibition and that coligation of BCR and CD72 is required for CD72-mediated signal regulation (Fig. 7 E) as is the case for other inhibitory co-receptors such as FcγRIIB (Muta et al., 1994). Thus, the epitope of BCR must be located on the ligand of CD72, i.e., Sm/RNP, to induce CD72 phosphorylation and CD72-mediated signal inhibition, resulting in specific down-modulation of the anti-Sm/RNP B cell response.

CD72 regulates antibody production to Sm/RNP

To address whether CD72 regulates antibody production to Sm/RNP, we immunized $CD72^{+/+}$ and $CD72^{-/-}$ mice with Sm/RNP or NP–chicken γ globulin (CGG) and measured titers of serum antibody to the immunized antigens. After immunization with Sm/RNP, anti-Sm/RNP IgG was not detected regardless of the genotype of mice. However, $CD72^{-/-}$ but not $CD72^{+/+}$ mice produced a significant amount of anti-Sm/RNP IgM (Fig. 8 B), and the ratio of anti-Sm/RNP IgM to total IgM was also significantly increased in $CD72^{-/-}$ but not $CD72^{+/+}$ mice (Fig. 8, A and C). In contrast, immunization with NP-CGG induced production of anti-NP IgM (Fig. 8 E) and IgG (Fig. 8 H) in both $CD72^{+/+}$ and $CD72^{-/-}$ mice. $CD72^{-/-}$ mice showed increased anti-NP IgM titer (Fig. 8 E), but the ratio of anti-NP IgM to total IgM was rather decreased in $CD72^{-/-}$ mice (Fig. 8, D and F), indicating that increased anti-NP IgM production in $CD72^{-/-}$ mice is caused by enhanced polyclonal IgM production but not enhanced specific antibody produc-

---

superposed on that of CD72^a CTLD (green). The bound carbohydrate chains are represented as a stick model. The Ca^{2+} ions for DC-SIGN and sulfate ions for EMBP are represented as a CPK model. The structures between the α2 helix and the β3 strand are colored as red (CD72^a) and black (other CTLDs). (G) Amino acid sequences of CTLDs of mouse CD72^a, mouse CD72^c, human CD72, human CD69, mouse dectin-1, human CD94, human DC-SIGN, and human EMBP are manually aligned based on their crystal structures. Among 17 groups of CTLDs classified on the basis of their domain organization and phylogeny, CD72, CD69, dectin-1, and CD94 are members of the group V CTLDs. DC-SIGN and EMBP belong to groups II and XII, respectively. The conserved cysteine residues are shown in yellow. The cysteine residues of CD72^a shown in orange are substituted by serine residues in CD72 CTLD proteins used for crystallographic study. The secondary structures of CD72^a CTLD are indicated above the sequences. Variable secondary structure regions between the α2 helix and β3 strand are highlighted as red (CD72^a) and gray (other CTLDs). The aromatic residues clustered at the L1 loop are shown in purple.
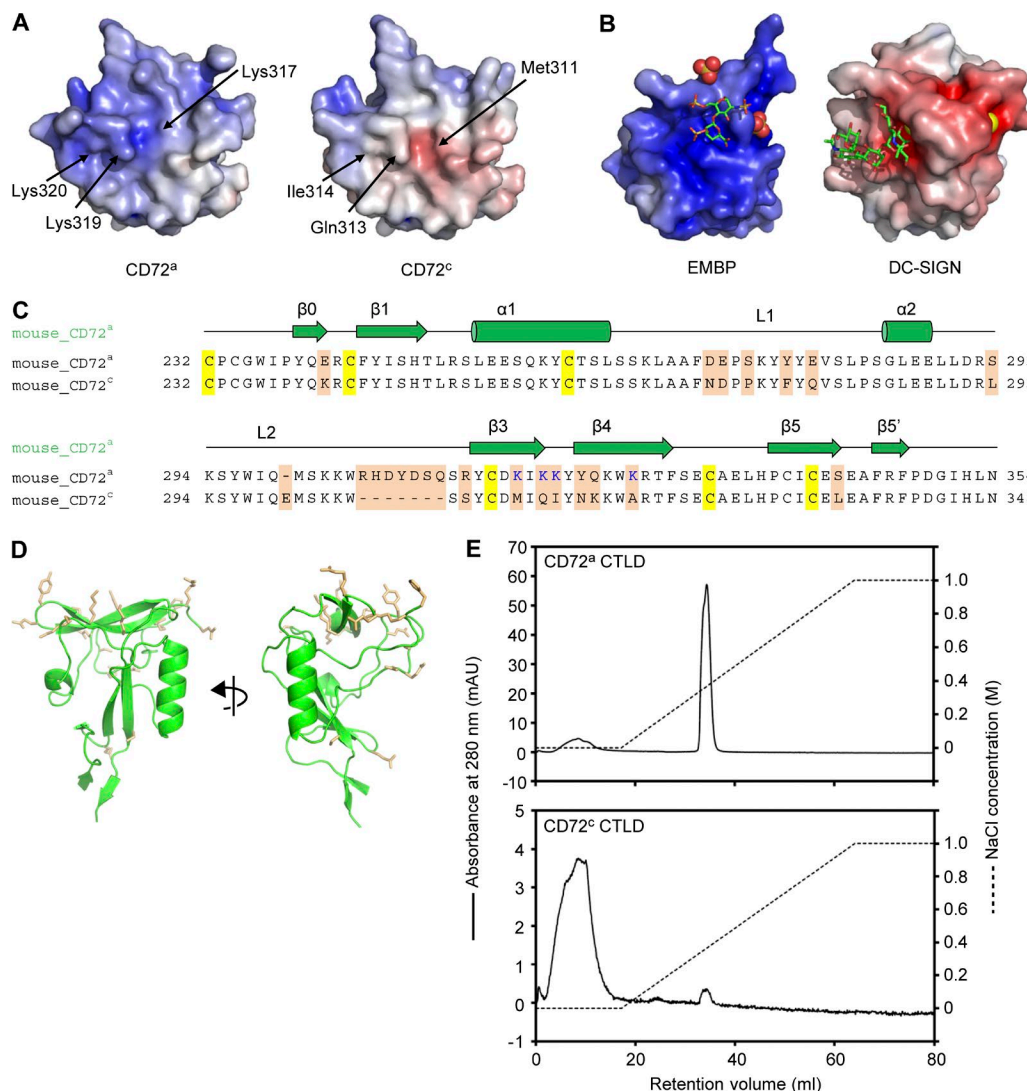
Figure 4. **Surface charge distribution of CD72[c] CTLD is different from that of CD72[a] CTLD.** (A and B) Electrostatic surface representation of CD72[a] and CD72[c] CTLDs (A) and EMBP and DC-SIGN (B) around the putative ligand-binding area. The viewpoint is the same as in Fig. 3 A (right). The color of the surface potentials is represented in the scale ranging from negatively (red) to positively (blue) charged. The positions of the substituted basic residues between CD72[a] and CD72[c] at the β3 strand are indicated by allows. The bound carbohydrates and ions (sulfate in EMBP and Ca^{2+} in DC-SIGN) are represented as stick and CPK models, respectively. (C) Amino acid sequence alignment of CD72[a] and CD72[c] CTLDs with the secondary structures of CD72[a] CTLD. Substituted residues are highlighted in orange. The basic residues at the β3 and β4 strands of CD72[a] shown in blue are substituted in CD72[c]. The conserved cysteine residues are shown in yellow. (D) Residues in CD72[a] CTLD, which are substituted in CD72[c] CTLD, are represented as the stick model (orange) in the structure of CD72[a] CTLD. (E) Elution profiles of CD72[a] and CD72[c] CTLD proteins on a cation exchange column. Proteins were eluted with a linear gradient of NaCl (0–1 M) in 50 mM Tris-HCl, pH 8.5. Representative data of two independent experiments are shown. mAU, milli–absorbance units.

tion. Moreover, production of anti-NP IgG was reduced in *CD72^{−/−}* mice (Fig. 8, G–I). Thus, CD72 specifically regulates antibody production to Sm/RNP.

DISCUSSION

Here, we demonstrated that recombinant CD72 CTLD specifically binds to the lupus-related nuclear self-antigen Sm/RNP using both ELISA and SPR. We also demonstrated that treatment with NP-Sm/RNP induced augmented

Ca^{2+} signaling, cell proliferation, and BCR endocytosis in *CD72^{−/−}* NP-reactive QM B cells compared with *CD72^{+/+}* QM B cells, whereas these B cell responses to NP-BSA were not augmented in *CD72^{−/−}* QM B cells. As interaction of NP-reactive B cells with NP-Sm/RNP and NP-BSA mimics that of Sm/RNP- and BSA-reactive B cells with the corresponding antigens, respectively (Fig. 5 A), this result suggests that B cell responses to Sm/RNP is specifically augmented in the absence of CD72. Moreover,
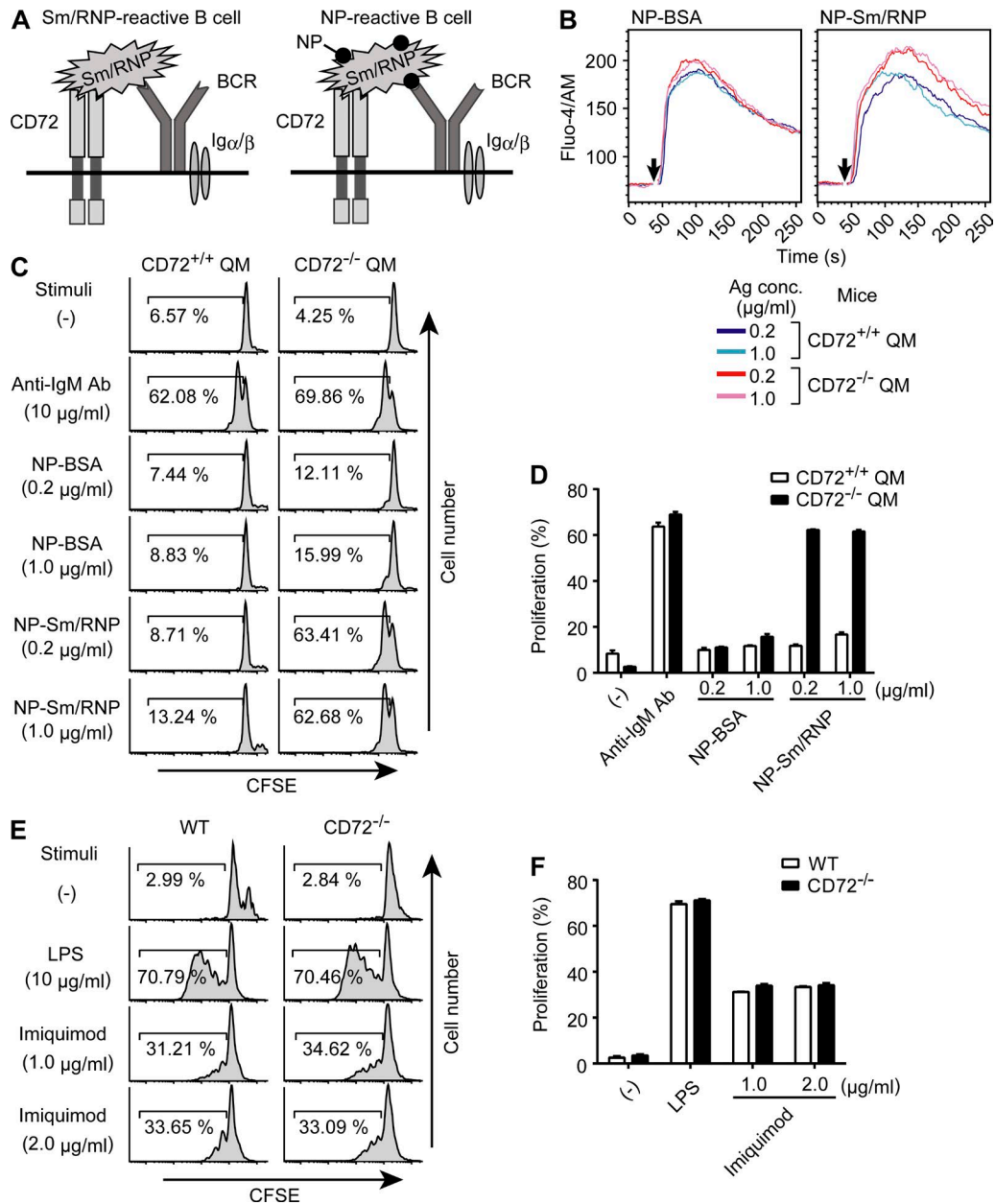
Figure 5. **CD72 specifically regulates B cell responses to Sm/RNP.** (A) Schematic representation of the experimental design to address B cell responses to Sm/RNP using anti–NP B cells and NP-Sm/RNP. Stimulation of anti–NP B cells from QM mice with NP-Sm/RNP (right) mimics that of anti–Sm/RNP B cells with Sm/RNP (left). (B) Ca^{2+} signaling. Fluo-4/AM–loaded spleen B cells from $CD72^{+/+}$ and $CD72^{-/-}$ QM mice were stimulated with the indicated concentrations (Ag conc.) of NP-BSA or NP-Sm/RNP, and the intracellular free calcium ion level was measured by flow cytometry for 300 s. The arrows indicate the time point when NP-BSA and NP-Sm/RNP were added. Data are representative of five independent experiments. (C–F) B cell proliferation. Purified B cells from $CD72^{+/+}$ and $CD72^{-/-}$ QM mice (C and D) or $CD72^{+/+}$ (WT) and $CD72^{-/-}$ C57BL/6 mice (E and F) were labeled with CFSE and cultured with indicated concentrations of anti-IgM, NP-BSA, and NP-Sm/RNP (C and D) or LPS and imiquimod (E and F) for 48 (C and D) or 72 (E and F) h. CFSE fluorescence was measured by flow cytometry. (C and E) The percentages of proliferated cells are indicated. (D and F) Mean ± SD of triplicates is shown. Data are representative of five independent experiments. Ab, antibody.

immunization with Sm/RNP induced autoantibody production to Sm/RNP in $CD72^{-/-}$ but not $CD72^{+/+}$ mice. Thus, the inhibitory receptor CD72 specifically down-regulates B cell responses to Sm/RNP.

We further demonstrated that coligation of BCR and CD72 is required for both phosphorylation and SHP-1 recruitment of CD72 (Fig. 7), the events essential for signal inhibition. This finding is in agreement with previous findings
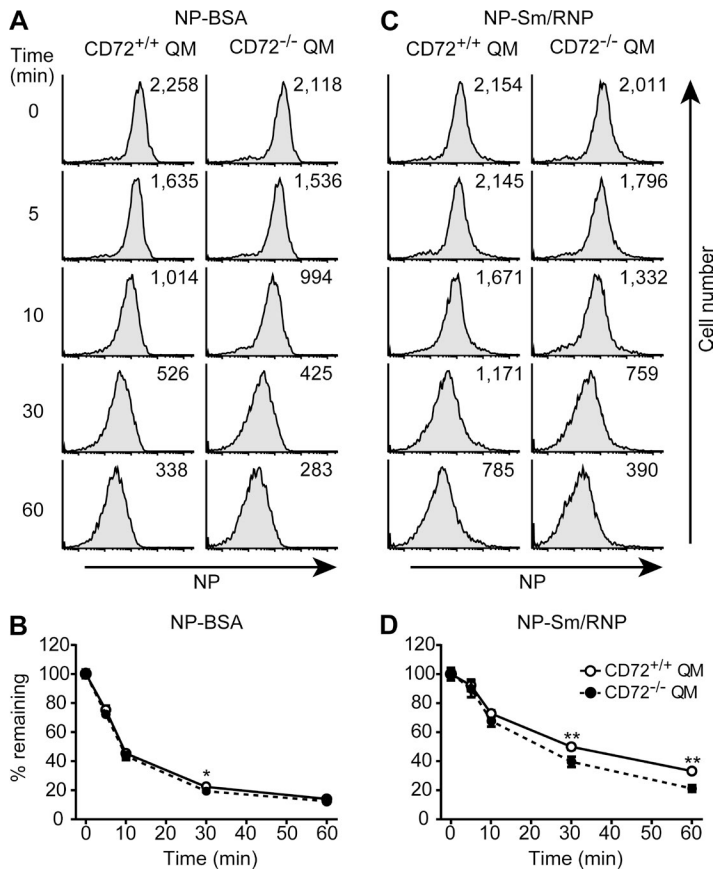
Figure 6. **CD72 specifically regulates endocytosis of Sm/RNP.** (A–D) Splenic B cells from *CD72^+/+* and *CD72^−/−* QM B cells were incubated with NP-BSA (A and B) or NP-Sm/RNP (C and D) on ice for 30 min. After washing, cells were incubated at 37°C for the indicated time and analyzed for remaining NP-BSA (A and B) and NP-Sm/RNP (C and D) on the cell surface by flow cytometry. (A and C) Mean fluorescence intensity is indicated. (B and D) Percentages of remaining NP-BSA (B) and NP-Sm/RNP (D) are calculated. Mean ± SD of triplicates is shown. Data are representative of four independent experiments. *, P < 0.05; **, P < 0.01 (two-tailed Student's *t* test).

with another inhibitory BCR co-receptor FcγRIIB (Muta et al., 1994). Because these co-receptors are phosphorylated at ITIMs by BCR–associated kinases such as Lyn (Adachi et al., 1998; Chan et al., 1998; Nishizumi et al., 1998), coligation of BCR and inhibitory co-receptors may allow their ITIMs access to the kinases. As coligation of BCR and CD72 is achieved only when Sm/RNP, the ligand of CD72, interacts with anti-Sm/RNP BCR, the requirement of coligation with BCR may restrict CD72 to specifically inhibit activation of anti-Sm/RNP B cells.

Here, we demonstrated that NP-Sm/RNP but not NP-BSA induces proliferation of anti-NP B cells in the absence of CD72, whereas both of these antigens fail to induce proliferation in the presence of CD72 (Fig. 5). This result indicates that Sm/RNP carries a stronger B cell activation capacity, which is abrogated by CD72. Sm/RNP that contains RNA is known to be an endogenous ligand for TLR7 (Lau et al., 2005), an RNA-recognizing TLR. As TLR7 is expressed in B cells as well as innate immune cells, Sm/RNP activates Sm/RNP-reactive B cells by inducing both BCR signaling and co-stimulatory signaling through TLR7 (Lau et al., 2005). Thus, Sm/RNP-reactive B cells tend to activation compared with B cells with other specificities, and this tendency appears to be involved in production of anti-Sm antibody that plays a crucial role in development of lupus (James et al., 1995; Berland et al., 2006; Christensen et al., 2006). This possibility is

supported by the findings that TLR7 is required for both production of anti-Sm antibody and development of lupus (Berland et al., 2006; Christensen et al., 2006). Our finding that CD72 negatively regulates B cell response to NP-Sm/RNP but not NP-BSA suggests that CD72 specifically counteracts to the tendency of activation in Sm/RNP-reactive B cells, thereby preventing development of lupus. Here, we further demonstrate that CD72 regulates B cell response to Sm/RNP but not a synthetic TLR7 ligand imiquimod. This suggests that CD72 regulates only response to Sm/RNP among various TLR7 ligands, probably because CD72 CTLD binds to Sm/RNP but not other TLR7 ligands, and does not appear to regulate TLR7-mediated responses to microbial RNA crucial for host defense to microbes (Diebold et al., 2004; Heil et al., 2004; Lund et al., 2004). Our findings thus suggest a crucial role of CD72 in immune homeostasis in which CD72 suppresses hazardous TLR7-mediated responses to the endogenous ligand Sm/RNP, which is an inevitable consequence of TLR7-mediated recognition of RNA, without influencing beneficial TLR7-medidated responses to microbial RNA.

CD72^−/− mice produce autoantibodies to various nuclear antigens such as DNA and histone as well as Sm/RNP (Xu et al., 2013) as is the case for patients with SLE, although we failed to show binding of CD72 CTLD to DNA or histone. However, a previous study demonstrated that immunization with Sm peptides induces production of autoantibodies
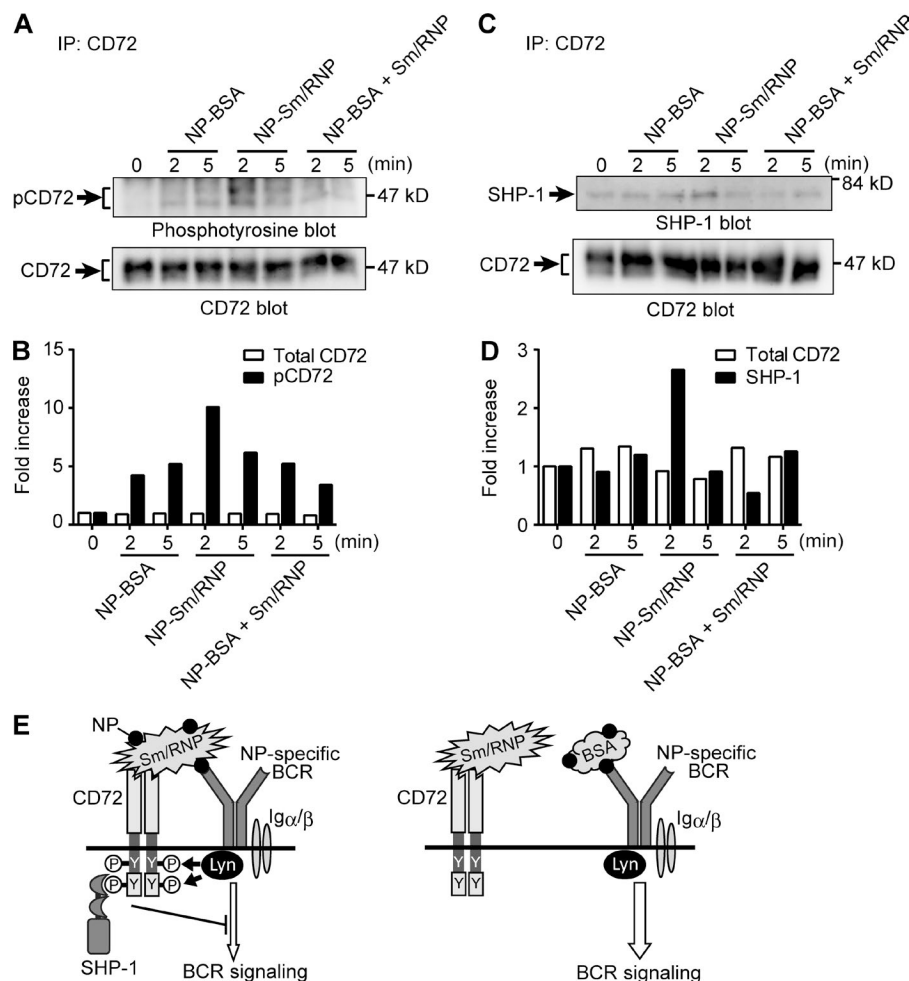
Figure 7. **NP-Sm/RNP induces phosphorylation and SHP-1 recruitment of CD72 in NP-reactive B cells.** (A–D) The B cell line BAL17-9T13 that expresses anti-NP BCR was treated with NP-BSA, NP-Sm/RNP, or a combination of NP-BSA and Sm/RNP for the indicated time, and lysates were immunoprecipitated (IP) with anti-CD72 antibody. Phosphorylated CD72 (pCD72; A) and SHP-1 (C) in the immunoprecipitates were analyzed by Western blotting. The intensities of protein bands for total CD72 (B and D), phosphorylated CD72 (B), and SHP-1 (D) were quantified and expressed as fold-change relative to unstimulated cells (0 min). Data are representative of four independent experiments. (E) Schematic representation of the mechanisms for CD72-mediated signal regulation. Coligation of CD72 with BCR mediated by Sm/RNP (left) but not independent ligation of CD72 and BCR (right) induces CD72 phosphorylation by BCR-associated kinases such as Lyn. The requirement of coligation restricts CD72-mediated signal inhibition only in Sm/RNP-reactive B cells. P, phosphate group; Y, tyrosine residue.

to Sm and also various other nuclear components including DNA and RNP in various animals, probably by the mechanism known as epitope spreading (Monneaux and Muller, 2002), and development of lupus-like disease in rabbits (James et al., 1995). Thus, CD72 deficiency causes autoimmune responses to various nuclear antigens other than Sm/RNP by epitope spreading resulting in production of antibodies to various nuclear antigens. Although anti-DNA antibody is produced in both human and mouse lupus, TLR9 involved in immune response to DNA-related antigens (Leadbetter et al., 2002) inhibits development of lupus (Christensen et al., 2006) probably by competing with TLR7 activity (Nickerson et al., 2010; Santiago-Raber et al., 2010). These findings suggest that autoimmune response to RNA- but not DNA-related antigens is dominant in regulation of development of lupus, although the mechanisms are not yet elucidated. CD72 appears to efficiently regulate lupus development by inhibiting B cell responses to Sm/RNP.

B cells express a variety of inhibitory receptors including CD72, which negatively regulates BCR signaling by activating phosphatases such as SHP-1 (Tsubata, 2012). Many of these inhibitory receptors including CD22 (Sgroi et al., 1993)

and PIR-B (Takai, 2005) recognize ubiquitous self-antigens such as sialic acids and MHC, respectively, and negatively regulate polyclonal BCR signaling induced by BCR ligation using anti–IgM antibody. Some of the mice deficient in one of these inhibitory receptors are lupus-prone (Tsubata, 2012), but the impact of the deficiency in inhibitory receptors other than CD72 in development of lupus is generally much weaker than that of CD72 deficiency. Indeed, deficiency in CD22 or PIR-B alone does not induce autoimmune disease (Jellusova et al., 2010; Takai et al., 2011), and development of autoimmune disease requires additional defect in Siglec-G or Fas, respectively (Kubo et al., 2009; Jellusova et al., 2010). The strong CD72-mediated regulation on lupus development was not supported by the previous findings on signal inhibition activity demonstrating that CD72 does not regulate polyclonal BCR signaling (Xu et al., 2013). However, the finding presented here that CD72 specifically regulates signaling through Sm/RNP-reactive BCR explains why CD72 strongly regulates development of the disease without affecting polyclonal BCR signaling. Thus, CD72 efficiently regulates development of lupus without affecting polyclonal B cell response by specifically regulating B cell response to
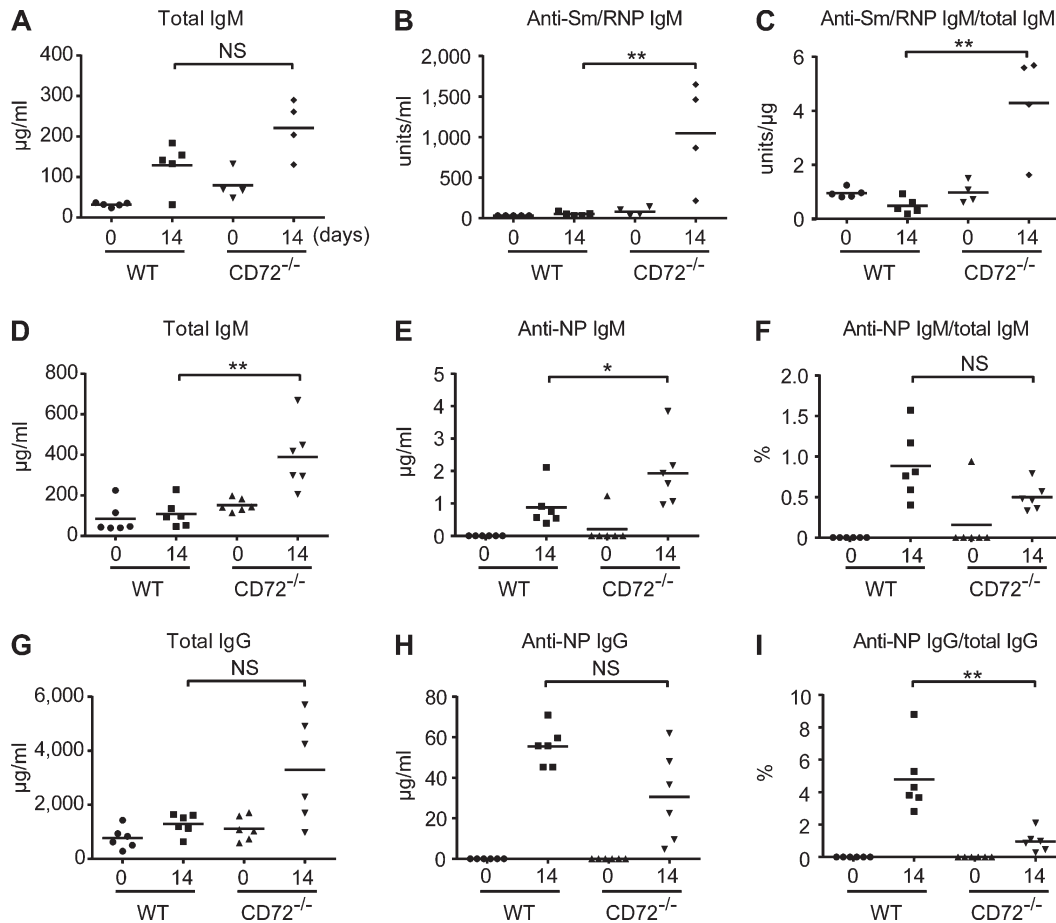
Figure 8.   **CD72 specifically regulates antibody production to Sm/RNP.** (A–I) WT and *CD72*⁻/⁻ female C57BL/6 mice (9 wk old) were immunized with Sm/RNP (*n* = 4–5 per group; A–C) and NP-CGG (*n* = 6 per group; D–I). After 14 d, serum levels of total IgM (A and D), total IgG (G), and titers of anti-Sm/RNP IgM (B), anti-NP IgM (E), and IgG (H) were measured by ELISA. Pooled MRL.*Fas*^lpr/lpr sera (1,000 U/ml), monoclonal anti-NP IgM B1-8, and anti-NP IgG C6 were used as standards to determine the titers of anti-Sm/RNP IgM and concentrations of anti-NP IgM and anti-NP IgG. (C, F, and I) The ratio of the amount of antigen-specific Ig to total Ig was calculated. *, P < 0.05; **, P < 0.01 (Brunner-Munzel test).

Sm/RNP, which plays a central role in the development of the disease. FcγRIIB is known as an inhibitory receptor that recognizes the disease-related self-antigen IgG, a target of rheumatoid factor. However, FcγRIIB regulates polyclonal B cells stimulated by anti-IgM and development of lupus (Nimmerjahn and Ravetch, 2008), although rheumatoid factor is typically produced in patients with rheumatoid arthritis. In contrast, CD72 specifically regulates self-reactive B cells by recognizing pathogenic lupus self-antigen, thereby efficiently preventing development of this disease.

Here, we demonstrated that CD72ᵃ CTLD binds to Sm/RNP with higher affinity than CD72ᶜ CTLD. The difference in affinity to Sm/RNP between CD72ᵃ CTLD and CD72ᶜ CTLD is modest as the K_D value of CD72ᶜ CTLD is only 50% higher than that of CD72ᵃ CTLD. However, there are examples such as FcγRIIA, FcγRIIIA (Bruhns et al., 2009; Gillis et al., 2014), and C3 (Heurich et al., 2011) in which a similar modest difference in affinity between different allelic

forms causes difference in biological responses and disease susceptibility. Thus, weaker binding of CD72ᶜ to Sm/RNP may compromise its regulation to prevent development of lupus-like disease and therefore explains our previous finding that CD72ᶜ is involved in development of severe lupus-like disease in MRL.*Fas*^lpr/lpr mice (Xu et al., 2013). As the impact of CD72ᶜ in development of the disease is much weaker than that of CD72 deficiency (Xu et al., 2013), modest reduction of affinity to Sm/RNP in CD72ᶜ may be attributed to the susceptibility of *CD72*ᶜ-carrying mice to lupus.

We have determined the crystal structure of CD72ᵃ CTLD at a very high resolution and, based on this structure, generated a homology model of CD72ᶜ CTLD. Because Sm/RNP is a large molecular complex composed of 11 peptides and 5 small RNAs, co-crystallization of CD72 with Sm/RNP would be very difficult. Thus, its ligand-binding site is still to be identified. Yet the electrostatic potentials of CD72ᵃ CTLD and CD72ᶜ CTLD provide an interesting

clue. A highly positively charged patch observed in the region containing the β3 and β4 strands, which is the ligand-biding site in some other CTLDs (Feinberg et al., 2001; Swaminathan et al., 2005), suggests that this region could be a binding site for negatively charged ligands. Because such patches are widely observed among the nucleic acid–binding proteins (Nadassy et al., 1999), it is tempting to speculate that it interacts in some way with the RNA component of Sm/RNP. This hypothesis is further supported by the presence of the aromatic–rich sequence (Y276, Y277, and Y278 in CD72[a]) at the edge of the positively charged patch because these aromatic residues may be preferred for the π-π stacking to nucleic acid bases (Wilson et al., 2014). Moreover, the fact that the same region of CD72[c] CTLD is negatively charged could explain why CD72[c] CTLD shows a lower affinity to Sm/RNP than CD72[a] CTLD does. On the other hand, our ELISA results clearly show single-stranded DNA (ssDNA) binds to neither CD72[a] CTLD nor CD72[c] CTLD (Fig. 1). In addition to the nucleic acid–mediated interaction, protein–protein interactions between CD72 CTLD and Sm/RNP may also contribute to the molecular recognition of Sm/RNP by CD72, by which CD72 may distinguish Sm/RNP from other TLR7 ligands.

In summary, we demonstrated here that the inhibitory B cell receptor CD72 recognizes the endogenous TLR7 ligand Sm/RNP and inhibits B cell response to this self-antigen. As TLR7-mediated response to Sm/RNP is crucial for development of lupus (James et al., 1995; Berland et al., 2006; Christensen et al., 2006), these results suggest that CD72 prevents development of lupus by inhibiting B cell response to Sm/RNP in agreement with the previous finding that CD72 deficiency efficiently causes lupus-like autoimmune disease in mice and also association of *CD72* polymorphism with SLE in both humans and mice.

MATERIALS AND METHODS
Mice
C57BL/6 mice were purchased from Sankyo Labo Service. *CD72−/−* mice (Xu et al., 2013) and QM mice (a gift from M. Wabl, University of California, San Francisco, CA) were described previously (Cascalho et al., 1996). All mice were bred and maintained in the animal facility of Tokyo Medical and Dental University under specific pathogen–free conditions. For immunization, 9-wk-old mice were intraperitoneally injected with 25 µg Sm/RNP (AroTec Diagnostics) or 100 µg NP17-CGG in 100 µl PBS mixed with an equal volume of complete Freund's adjuvant (Sigma-Aldrich) or 10 µg LPS (Sigma-Aldrich), respectively. Experiments were approved by the Institutional Animal Care and Use Committee of Tokyo Medical and Dental University and were performed according to our institutional guidelines.

Plasmids
The DNA fragments encoding CTLD of CD72[a] (residues 232–354) and CD72[c] (residues 232–348) were generated by RT-PCR and cloned into NdeI/EcoRI-opened pET-28a plasmid (EMD Millipore), followed by insertion of the synthetic oligonucleotides encoding the Avi-tag sequence (Schatz, 1993; Beckett et al., 1999) into the NcoI site (pET28aAviCD72[a]CTLD and pET28cAviCD72[c]CTLD, respectively). Alternatively, the DNA fragments encoding CTLD of CD72[a] C234S/C338S (CD72[a] CTLDc/s) mutant and CTLD of CD72[c] C234S/C332S (CD72[c] CTLDc/s) mutant were generated by RT-PCR and inverted PCR and cloned into NdeI/SalI-opened pET-28a (pET28aCD72[a] CTLDc/s and pET28cCD72[c]CTLDc/s, respectively).

Reagents
NP-conjugated CGG, NP-conjugated BSA, and NP-conjugated Sm/RNP were prepared as described previously (Oda and Azuma, 2000) with some modifications. In brief, hydroxysuccinimide ester of NP (NP-OSu) was generated by incubating 50 mM NP (Alfa Aesar) in 1,4-dioxane with 150 mM *N*-hydroxysuccinimide (Wako Pure Chemical Industries) and 50 mM *N,N'*-dicyclohexylcarbodiimide (Wako Pure Chemical Industries) at 37°C overnight. NP-OSu was incubated with CGG (Rockland Immunochemicals), BSA, or Sm/RNP in 0.2 M NaHCO₃-NaOH buffer, pH 9.0, at room temperature overnight. After dialysis against PBS, pH 7.4, concentrations of NP, CGG, BSA, and Sm/RNP were determined by spectrophotometry, and the conjugation ratios of NP per CGG, BSA, and Sm/RNP were determined. NP15-BSA and NP-Sm/RNP, in which Sm/RNP was conjugated by 47% more NP than NP-BSA by weight ratio, were used for stimulation of B cells in this study.

Recombinant CD72 CTLD proteins
For generation of biotinylated CD72 CTLD proteins, BL21AI cells (Invitrogen) were transformed with pBirAcm encoding the biotin ligase BirA (BL21AI-BirA) and maintained in the presence of 10 µg/ml chloramphenicol. BL21AI-BirA was transformed with pET28aAviCD72[a]CTLD or pET28aAviCD72[c]CTLD and cultured in the presence of 50 µM biotin, 1 mM isopropyl β-D-thiogalactopyranoside, 0.2% arabinose, 50 µg/ml kanamycin, and 10 µg/ml chloramphenicol. For generation of CD72 CTLD proteins for crystallization and SPR, BL21DE3 (Invitrogen) was transformed with pET28aCD72[a]CTLDc/s and pET28cCD72[c]CTLDc/s and was cultured in Luria–Bertani medium containing 1 mM isopropyl β-D-thiogalactopyranoside and kanamycin. The cells were suspended in a buffer containing 50 mM Tris-HCl, pH 8.0, 300 mM NaCl, and 0.5% (vol/vol) Triton X-100 and sonicated on ice. After centrifugation, the inclusion bodies were washed in 50 mM Tris-HCl, pH 8.0, and 300 mM NaCl. The washed inclusion bodies were resuspended in the solubilization buffer containing 50 mM Tris-HCl, pH 8.0, 500 mM NaCl, 6 M guanidine hydrochloride, and 40 mM dithiothreitol and completely denatured through overnight incubation at 37°C. Then, the concentration of dithiothreitol was reduced to 20 mM, and the protein solution was applied onto

a column of 50 ml His–Accept SF resin (Nacalai Tesque). Refolding of the bound protein was performed using a refolding buffer containing 50 mM Tris-HCl, pH 8.5, 400 mM NaCl, 500 mM L-arginine hydrochloride, 10% (vol/vol) glycerol, 5 mM reduced glutathione, and 0.5 mM oxidized glutathione. The column was washed with 150 ml of the refolding buffer at a low flow rate (0.5 ml/min) and then the wash solution containing 50 mM Tris-HCl, pH 8.0, and 400 mM NaCl in the same way as the refolding buffer. The refolded protein was eluted with the elution buffer containing 50 mM Tris-HCl, pH 8.0, 300 mM NaCl, and 400 mM imidazole. The eluted fraction was dialyzed against a buffer containing 20 mM Tris-HCl, pH 8.0, and 300 mM NaCl at 4°C. CD72CTLDc/s proteins were treated with thrombin protease (GE Healthcare) at 20°C overnight to remove the hexahistidine tag. The cleaved protein was applied onto a Superdex 200 prep grade column (HiLoad 26/600; GE Healthcare) equilibrated with a buffer containing 20 mM Tris-HCl, pH 8.0, and 300 mM NaCl. The fraction of the monomer CD72[a] CTLD was concentrated to 5–10 mg/ml at 25°C just before crystallization experiments to avoid forming aggregation.

ELISA

ssDNA was prepared by heat denaturing calf thymus DNA (Sigma-Aldrich). ELISA plates (Nunc-Immuno 96 MicroWell Plate; PolySorp; Thermo Fisher Scientific) were coated with 10 µg/ml ssDNA, histone, cardiolipin, Sm/RNP (AroTec Diagnostics), or NP$_6$-BSA. ELISA plates were then blocked with PBS containing 1% BSA. Recombinant biotinylated CD72 CTLD proteins were added to the ELISA plates and detected by alkaline phosphatase–conjugated streptavidin (BD). Alternatively, ELISA plates were incubated with mouse sera, washed, and reacted with alkaline phosphatase–conjugated anti–mouse IgM (SouthernBiotech) or IgG antibody (SouthernBiotech). After washing, ELISA plates were reacted with phosphatase substrate (Sigma-Aldrich), and absorbance at 405 nm was measured on a Vmax kinetic microplate reader (Molecular Devices). For competitive ELISA, Sm/RNP-coated ELISA plates were incubated with a mixture of recombinant biotinylated CD72[c] CTLD protein (0.5 or 1 µg/ml) and serially diluted nonbiotinylated CD72[a] CTLDc/s or CD72[c] CTLDc/s recombinant proteins as competitors. The bound biotinylated CD72[c] CTLD proteins were detected by alkaline phosphatase–conjugated streptavidin (BD). Total mouse IgM and IgG in mouse sera were determined by standard sandwich ELISA.

SPR measurements

SPR analysis was done using a BIAcore T100 system (GE Healthcare). 14 µM CD72[a] CTLDc/s and 15 µM CD72[c] CTLDc/s recombinant proteins in 10 mM 2-(N-morpholino) ethanesulfonic acid, pH 6.0, were covalently immobilized on a CM5 sensor chip (GE Healthcare) to the level of more than 5,000 resonance units by amine coupling methods using a standard amine coupling kit (GE Healthcare). A control surface was prepared by activating and blocking a CM5 sensor tip with 1 M ethanolamine without protein. Various concentrations of Sm/RNP were injected over sensor chips at a flow rate of 30 µl/min. An association step of 120 s was followed by a dissociation step of 120 s. Responses to Sm/RNP were corrected by the responses with a control surface and those from a buffer only injection. Data were analyzed by BIAcore T100 Evaluation software (version 2.0.2; GE Healthcare) using a 1:1 binding model.

Cell culture

Mouse spleen B cells were prepared as described previously (Nomura et al., 1996). Cells were labeled with 2 µM CFSE (Molecular Probes) for 10 min. 2×10^5 CFSE-labeled cells were cultured in 200 µl RPMI 1640 medium (Wako Pure Chemical Industries) supplemented with 10% FCS (Nichirei Biosciences), 50 µM 2-mercaptoethanol (Sigma), and 1% penicillin/streptomycin (Nacalai Tesque) in a 96-well plate with F(ab')$_2$ fragments of goat anti–mouse IgM antibody (Jackson ImmunoResearch Laboratories, Inc.), NP-BSA, NP-Sm/RNP, imiquimod (InvivoGen), or LPS (Sigma-Aldrich). After 48 or 72 h, cells were analyzed by flow cytometry using FACS Verse flow cytometer (BD). For endocytosis assay, cells were incubated with 1 µg/ml NP-BSA or NP-Sm/RNP on ice for 30 min. After washing, 2×10^5 cells in 100 µl complete culture medium were incubated at 37°C for various time. The reaction was terminated by addition of ice-cold PBS containing 2% FCS. Cells were stained with biotinylated anti-NP antibody (C6; a gift from Y. Takahashi, National Institute of Infectious Diseases, Tokyo, Japan) together with Alexa Fluor 647–conjugated streptavidin (Molecular Probes) and analyzed by FACS Verse flow cytometer (BD).

Measurement of intracellular Ca²⁺ concentration

2×10^6 cells were incubated with 5 µg/ml Fluo-4/AM (Invitrogen) for 30 min. After washing, cells were stimulated with NP-BSA or NP-Sm/RNP. Fluo-4 fluorescence was measured continuously using a FACS Calibur cell analyzer (BD). Data were analyzed by FlowJo (Tree Star).

Immunoprecipitation and Western blotting

BAL17-9T13 cells were generated by introducing cDNAs encoding heavy and light chains of anti–NP antibody 9T13 (Furukawa et al., 1999) into the B cell line BAL17 (a gift from K. Takatsu, University of Tokyo, Tokyo, Japan). Mycoplasma contamination was not tested. Cells were stimulated with 5 µg/ml NP-BSA, 5 µg/ml NP-Sm/RNP, or a combination of 5 µg/ml NP-BSA and 5 µg/ml Sm/RNP and lysed in Triton X-100 lysis buffer (1% Triton X-100, 10% glycerol, 150 mM sodium chloride, 20 mM Tris-HCl, 2 mM EDTA, 0.02% sodium azide, 10 µg/ml PMSF, and 1 mM sodium orthovanadate). Lysates were immunoprecipitated with anti-CD72 antibody K10.6 (a gift from N. Tada, Tokai University, Tokyo, Japan; Tada et al., 1981) using protein G–sepharose (GE Healthcare). Immunoprecipitates

were separated by SDS-PAGE and transferred to polyvinylidene fluoride membranes (EMD Millipore). Membranes were incubated with anti-phosphotyrosine antibody pTyr102 (Cell Signaling Technology) together with HRP-conjugated rabbit anti–mouse IgG1 (SouthernBiotech) and rabbit anti-CD72 antibody (Santa Cruz Biotechnology, Inc.), followed by incubation with HRP-conjugated anti–rabbit IgG (Invitrogen). Alternatively, membranes were incubated with rabbit anti–mouse CD72 (Santa Cruz Biotechnology, Inc.) or rabbit anti–SHP-1 antibody (Santa Cruz Biotechnology, Inc.) followed by reaction with HRP-conjugated anti–rabbit IgG (Invitrogen). Proteins were then visualized using Chemi-Lumi One L (Nacalai Tesque). The intensity of protein bands was quantified using ImageQuant TL software (GE Healthcare).

Crystallization and structure analyses

Crystals of CD72[a] CTLD were obtained with the hanging-drop vapor-diffusion method at 20°C by mixing 1 µl of protein solution with 1 µl of reservoir solution containing 100 mM imidazole, pH 6.5, 1 M sodium acetate trihydrate, and 10 mM hexamine cobalt (III) chloride. Well-shaped hexagonal rod-like crystals grew within 7 d to a maximum length of 0.6 mm. Before data collection, the crystals were soaked in a solution containing 20% (vol/vol) glycerol and crystallization reagents and flash cooled under a nitrogen gas stream at 95 K. X-ray diffraction experiments were performed at beamlines BL-5A, BL-17A, and NW12A in KEK-PF and BL26B1 and BL38B1 in SPring-8. The data were processed and scaled using HKL2000 (Otwinowski and Minor, 1997) and truncated by the CCP4 program suite (Winn et al., 2011). Initial phases were obtained by molecular replacement using PHASER (McCoy et al., 2007) with the structure of human CD69 (PDB accession no. 1FM5; Natarajan et al., 2000) as a search model. Several cycles of manual model rebuilding and refinement were performed by using COOT (Emsley et al., 2010), REFMAC (Murshudov et al., 2011), and PHENIX (Adams et al., 2010). The refined models were validated by the program MOLPROBITY (Chen et al., 2010). The statistics for data collection and refinement are summarized in Table 1. The protein homology model was built by SWISS-MODEL Workspace (Biasini et al., 2014). All structural illustrations were prepared with the program PYMOL. Structure-based amino acid sequence alignments (Fig. 3 G) were prepared using the sequences of the CTLDs of mouse CD72[a], mouse CD72[c] (Tung et al., 1986; Robinson et al., 1992; Powell et al., 1995), human CD72 (Von Hoegen et al., 1990), human CD69 (Natarajan et al., 2000), mouse dectin-1 (Brown et al., 2007), human CD94 (Boyington et al., 1999), human DC-SIGN (Feinberg et al., 2001), and human EMBP (Swaminathan et al., 2005). Structural comparison of CD72[a] and other CTLDs were done using crystal structures of human CD69 (Natarajan et al., 2000), mouse dectin-1 (Brown et al., 2007), human CD94 (Boyington et al., 1999), human DC-SIGN (Feinberg et al., 2001), and human EMBP (Swaminathan et al., 2005).

Cation exchange column chromatography

0.5 mg CD72[a] and 0.06 mg CD72[c] CTLD proteins in 4 ml 50 mM Tris-HCl, pH 8.5, were applied onto a 5-ml cation exchange column (HiTrap SP HP; GE Healthcare) equilibrated with the same buffer. The proteins were eluted with the linear gradient from 0 to 1 M NaCl within 10-column volumes.

Statistical analysis

Data of in vitro experiments were analyzed by unpaired two-tailed Student's t tests after equality of variance was determined by an F test. Analysis was done using PRISM (GraphPad Software). Data of in vivo immunization were analyzed by nonparametrical Brunner-Munzel test that allows for unequal variances using the R software. P-values <0.05 were regarded as statistically significant.

Data access

Coordinates and structure factors have been deposited in PDB under accession no. 5B1R.

Table 1. **Data collection and refinement statistics for x-ray crystallographic analysis**

Statistics	CD72[a] CTLD
Data collection	
Wavelength (Å)	0.9800
Space group	$P6_1$
Unit-cell parameters (Å)	a = 65.5; c = 61.2
Resolution (Å)	50–1.20 (1.22–1.20)[a]
No. of observations	510,694
No. of unique reflections	46,533
Completeness (%)	99.8 (100)
Average $I/\sigma(I)$	42.8 (4.1)
Redundancy	11.0 (10.6)
R_{sym}[b] (%)	8.7 (79.4)
Refinement	
R[c] (%)	12.8
R_{free}[d] (%)	14.8
Number of atoms	
Protein	1,003
Heterogen	10
Water	170
Average B factor (Å²)	18.0
Root-mean-square deviation from ideal	
Bonds (Å)	0.008
Angles (°)	1.21
Ramachandran plot	
Favored region (%)	97.4
Allowed region (%)	2.6
Outlier region (%)	0

[a]Values in parentheses are for the highest-resolution shell.

[b]$R_{sym} = \Sigma\Sigma_i|I(h) - I(h)_i|/\Sigma\Sigma_i I(h)$, where $I(h)$ is the mean intensity after rejection.

[c]$R = \Sigma|F_o - F_c|/\Sigma|F_o|$, where F_o is the observed structure factor amplitude and F_c is the calculated structure factor amplitude.

[d]R_{free} is the same as R but was calculated using a random set containing 5% of the data that were excluded during refinement.

JEM

REFERENCES

Adachi, T., H. Flaswinkel, H. Yakura, M. Reth, and T. Tsubata. 1998. The B cell surface protein CD72 recruits the tyrosine phosphatase SHP-1 upon tyrosine phosphorylation. *J. Immunol.* 160:4662–4665.

Adachi, T., C. Wakabayashi, T. Nakayama, H. Yakura, and T. Tsubata. 2000. CD72 negatively regulates signaling through the antigen receptor of B cells. *J. Immunol.* 164:1223–1229. http://dx.doi.org/10.4049/jimmunol.164.3.1223

Adams, P.D., P.V. Afonine, G. Bunkóczi, V.B. Chen, I.W. Davis, N. Echols, J.J. Headd, L.W. Hung, G.J. Kapral, R.W. Grosse-Kunstleve, et al. 2010. PHENIX: a comprehensive Python-based system for macromolecular structure solution. *Acta Crystallogr. D Biol. Crystallogr.* 66:213–221. http://dx.doi.org/10.1107/S0907444909052925

Beckett, D., E. Kovaleva, and P.J. Schatz. 1999. A minimal peptide substrate in biotin holoenzyme synthetase-catalyzed biotinylation. *Protein Sci.* 8:921–929. http://dx.doi.org/10.1110/ps.8.4.921

Berland, R., L. Fernandez, E. Kari, J.H. Han, I. Lomakin, S. Akira, H.H. Wortis, J.F. Kearney, A.A. Ucci, and T. Imanishi-Kari. 2006. Toll-like receptor 7-dependent loss of B cell tolerance in pathogenic autoantibody knockin mice. *Immunity.* 25:429–440. http://dx.doi.org/10.1016/j.immuni.2006.07.014

Biasini, M., S. Bienert, A. Waterhouse, K. Arnold, G. Studer, T. Schmidt, F. Kiefer, T. Gallo Cassarino, M. Bertoni, L. Bordoli, and T. Schwede. 2014. SWISS-MODEL: modelling protein tertiary and quaternary structure using evolutionary information. *Nucleic Acids Res.* 42:W252–W258. http://dx.doi.org/10.1093/nar/gku340

Boyington, J.C., A.N. Riaz, A. Patamawenu, J.E. Coligan, A.G. Brooks, and P.D. Sun. 1999. Structure of CD94 reveals a novel C-type lectin fold: implications for the NK cell-associated CD94/NKG2 receptors. *Immunity.* 10:75–82. http://dx.doi.org/10.1016/S1074-7613(00)80008-4

Brown, J., C.A. O'Callaghan, A.S. Marshall, R.J. Gilbert, C. Siebold, S. Gordon, G.D. Brown, and E.Y. Jones. 2007. Structure of the fungal β-glucan-binding immune receptor dectin-1: implications for function. *Protein Sci.* 16:1042–1052. http://dx.doi.org/10.1110/ps.072791207

Bruhns, P., B. Iannascoli, P. England, D.A. Mancardi, N. Fernandez, S. Jorieux, and M. Daëron. 2009. Specificity and affinity of human Fcγ receptors and their polymorphic variants for human IgG subclasses. *Blood.* 113:3716–3725. http://dx.doi.org/10.1182/blood-2008-09-179754

Cascalho, M., A. Ma, S. Lee, L. Masat, and M. Wabl. 1996. A quasi-monoclonal mouse. *Science.* 272:1649–1652. http://dx.doi.org/10.1126/science.272.5268.1649

Chan, V.W., C.A. Lowell, and A.L. DeFranco. 1998. Defective negative regulation of antigen receptor signaling in Lyn-deficient B lymphocytes. *Curr. Biol.* 8:545–553. http://dx.doi.org/10.1016/S0960-9822(98)70223-4

Chen, V.B., W.B. Arendall III, J.J. Headd, D.A. Keedy, R.M. Immormino, G.J. Kapral, L.W. Murray, J.S. Richardson, and D.C. Richardson. 2010. MolProbity: all-atom structure validation for macromolecular crystallography. *Acta Crystallogr. D Biol. Crystallogr.* 66:12–21. http://dx.doi.org/10.1107/S0907444909042073

Christensen, S.R., J. Shupe, K. Nickerson, M. Kashgarian, R.A. Flavell, and M.J. Shlomchik. 2006. Toll-like receptor 7 and TLR9 dictate autoantibody specificity and have opposing inflammatory and regulatory roles in a murine model of lupus. *Immunity.* 25:417–428. http://dx.doi.org/10.1016/j.immuni.2006.07.013

Diebold, S.S., T. Kaisho, H. Hemmi, S. Akira, and C. Reis e Sousa. 2004. Innate antiviral responses by means of TLR7-mediated recognition of single-stranded RNA. *Science.* 303:1529–1531. http://dx.doi.org/10.1126/science.1093616

Emsley, P., B. Lohkamp, W.G. Scott, and K. Cowtan. 2010. Features and development of Coot. *Acta Crystallogr. D Biol. Crystallogr.* 66:486–501. http://dx.doi.org/10.1107/S0907444910007493

Feinberg, H., D.A. Mitchell, K. Drickamer, and W.I. Weis. 2001. Structural basis for selective recognition of oligosaccharides by DC-SIGN and DC-SIGNR. *Science.* 294:2163–2166. http://dx.doi.org/10.1126/science.1066371

Furukawa, K., A. Akasako-Furukawa, H. Shirai, H. Nakamura, and T. Azuma. 1999. Junctional amino acids determine the maturation pathway of an antibody. *Immunity.* 11:329–338. http://dx.doi.org/10.1016/S1074-7613(00)80108-9

Gillis, C., A. Gouel-Chéron, F. Jönsson, and P. Bruhns. 2014. Contribution of human FcγRs to disease with evidence from human polymorphisms and transgenic animal studies. *Front. Immunol.* 5:254. http://dx.doi.org/10.3389/fimmu.2014.00254

Heil, F., H. Hemmi, H. Hochrein, F. Ampenberger, C. Kirschning, S. Akira, G. Lipford, H. Wagner, and S. Bauer. 2004. Species-specific recognition of single-stranded RNA via toll-like receptor 7 and 8. *Science.* 303:1526–1529. http://dx.doi.org/10.1126/science.1093620

Hemmi, H., T. Kaisho, O. Takeuchi, S. Sato, H. Sanjo, K. Hoshino, T. Horiuchi, H. Tomizawa, K. Takeda, and S. Akira. 2002. Small anti-viral compounds activate immune cells via the TLR7 MyD88-dependent signaling pathway. *Nat. Immunol.* 3:196–200. http://dx.doi.org/10.1038/ni758

Heurich, M., R. Martínez-Barricarte, N.J. Francis, D.L. Roberts, S. Rodríguez de Córdoba, B.P. Morgan, and C.L. Harris. 2011. Common polymorphisms in C3, factor B, and factor H collaborate to determine systemic complement activity and disease risk. *Proc. Natl. Acad. Sci. USA.* 108:8761–8766. http://dx.doi.org/10.1073/pnas.1019338108

Hitomi, Y., N. Tsuchiya, A. Kawasaki, J. Ohashi, T. Suzuki, C. Kyogoku, T. Fukazawa, S. Bejrachandra, U. Siriboonrit, D. Chandanayingyong, et al. 2004. *CD72* polymorphisms associated with alternative splicing modify susceptibility to human systemic lupus erythematosus through epistatic interaction with *FCGR2B.* *Hum. Mol. Genet.* 13:2907–2917. http://dx.doi.org/10.1093/hmg/ddh318

Izui, S., V.E. Kelley, K. Masuda, H. Yoshida, J.B. Roths, and E.D. Murphy. 1984. Induction of various autoantibodies by mutant gene lpr in several strains of mice. *J. Immunol.* 133:227–233.

James, J.A., T. Gross, R.H. Scofield, and J.B. Harley. 1995. Immunoglobulin epitope spreading and autoimmune disease after peptide immunization: Sm B/B'-derived PPPGMRPP and PPPGIRGP induce spliceosome autoimmunity. *J. Exp. Med.* 181:453–461. http://dx.doi.org/10.1084/jem.181.2.453

Jellusova, J., U. Wellmann, K. Amann, T.H. Winkler, and L. Nitschke. 2010. CD22 × Siglec-G double-deficient mice have massively increased B1

2704

CD72 negatively regulates anti-Sm/RNP B cells | Akatsu et al.

cell numbers and develop systemic autoimmunity. *J. Immunol.* 184:3618–3627. http://dx.doi.org/10.4049/jimmunol.0902711

Kubo, T., Y. Uchida, Y. Watanabe, M. Abe, A. Nakamura, M. Ono, S. Akira, and T. Takai. 2009. Augmented TLR9-induced Btk activation in PIR-B–deficient B-1 cells provokes excessive autoantibody production and autoimmunity. *J. Exp. Med.* 206:1971–1982. http://dx.doi.org/10.1084/jem.20082392

Lau, C.M., C. Broughton, A.S. Tabor, S. Akira, R.A. Flavell, M.J. Mamula, S.R. Christensen, M.J. Shlomchik, G.A. Viglianti, I.R. Rifkin, and A. Marshak-Rothstein. 2005. RNA-associated autoantigens activate B cells by combined B cell antigen receptor/Toll-like receptor 7 engagement. *J. Exp. Med.* 202:1171–1177. http://dx.doi.org/10.1084/jem.20050630

Leadbetter, E.A., I.R. Rifkin, A.M. Hohlbaum, B.C. Beaudette, M.J. Shlomchik, and A. Marshak-Rothstein. 2002. Chromatin-IgG complexes activate B cells by dual engagement of IgM and Toll-like receptors. *Nature.* 416:603–607. http://dx.doi.org/10.1038/416603a

Li, D.H., M.M. Winslow, T.M. Cao, A.H. Chen, C.R. Davis, E.D. Mellins, P.J. Utz, G.R. Crabtree, and J.R. Parnes. 2008. Modulation of peripheral B cell tolerance by CD72 in a murine model. *Arthritis Rheum.* 58:3192–3204. http://dx.doi.org/10.1002/art.23812

Lund, J.M., L. Alexopoulou, A. Sato, M. Karow, N.C. Adams, N.W. Gale, A. Iwasaki, and R.A. Flavell. 2004. Recognition of single-stranded RNA viruses by Toll-like receptor 7. *Proc. Natl. Acad. Sci. USA.* 101:5598–5603. http://dx.doi.org/10.1073/pnas.0400937101

Malhotra, S., S. Kovats, W. Zhang, and K.M. Coggeshall. 2009. B cell antigen receptor endocytosis and antigen presentation to T cells require Vav and dynamin. *J. Biol. Chem.* 284:24088–24097. http://dx.doi.org/10.1074/jbc.M109.014209

McCoy, A.J., R.W. Grosse-Kunstleve, P.D. Adams, M.D. Winn, L.C. Storoni, and R.J. Read. 2007. Phaser crystallographic software. *J. Appl. Cryst.* 40:658–674. http://dx.doi.org/10.1107/S0021889807021206

Monneaux, F., and S. Muller. 2002. Epitope spreading in systemic lupus erythematosus: identification of triggering peptide sequences. *Arthritis Rheum.* 46:1430–1438. http://dx.doi.org/10.1002/art.10263

Murshudov, G.N., P. Skubák, A.A. Lebedev, N.S. Pannu, R.A. Steiner, R.A. Nicholls, M.D. Winn, F. Long, and A.A. Vagin. 2011. REFMAC5 for the refinement of macromolecular crystal structures. *Acta Crystallogr. D Biol. Crystallogr.* 67:355–367. http://dx.doi.org/10.1107/S0907444911001314

Muta, T., T. Kurosaki, Z. Misulovin, M. Sanchez, M.C. Nussenzweig, and J.V. Ravetch. 1994. A 13-amino-acid motif in the cytoplasmic domain of FcγRIIB modulates B-cell receptor signalling. *Nature.* 368:70–73. http://dx.doi.org/10.1038/368070a0

Nadassy, K., S.J. Wodak, and J. Janin. 1999. Structural features of protein-nucleic acid recognition sites. *Biochemistry.* 38:1999–2017. http://dx.doi.org/10.1021/bi982362d

Natarajan, K., M.W. Sawicki, D.H. Margulies, and R.A. Mariuzza. 2000. Crystal structure of human CD69: a C-type lectin-like activation marker of hematopoietic cells. *Biochemistry.* 39:14779–14786. http://dx.doi.org/10.1021/bi0018180

Nickerson, K.M., S.R. Christensen, J. Shupe, M. Kashgarian, D. Kim, K. Elkon, and M.J. Shlomchik. 2010. TLR9 regulates TLR7- and MyD88-dependent autoantibody production and disease in a murine model of lupus. *J. Immunol.* 184:1840–1848. http://dx.doi.org/10.4049/jimmunol.0902592

Nimmerjahn, F., and J.V. Ravetch. 2008. Fcγ receptors as regulators of immune responses. *Nat. Rev. Immunol.* 8:34–47. http://dx.doi.org/10.1038/nri2206

Nishizumi, H., K. Horikawa, I. Mlinaric-Rascan, and T. Yamamoto. 1998. A double-edged kinase Lyn: a positive and negative regulator for antigen receptor-mediated signals. *J. Exp. Med.* 187:1343–1348. http://dx.doi.org/10.1084/jem.187.8.1343

Nitschke, L., and T. Tsubata. 2004. Molecular interactions regulate BCR signal inhibition by CD22 and CD72. *Trends Immunol.* 25:543–550. http://dx.doi.org/10.1016/j.it.2004.08.002

Nitschke, L., R. Carsetti, B. Ocker, G. Köhler, and M.C. Lamers. 1997. CD22 is a negative regulator of B-cell receptor signalling. *Curr. Biol.* 7:133–143. http://dx.doi.org/10.1016/S0960-9822(06)00057-1

Nomura, T., H. Han, M.C. Howard, H. Yagita, H. Yakura, T. Honjo, and T. Tsubata. 1996. Antigen receptor–mediated B cell death is blocked by signaling via CD72 or treatment with dextran sulfate and is defective in autoimmunity-prone mice. *Int. Immunol.* 8:867–875. http://dx.doi.org/10.1093/intimm/8.6.867

Oda, M., and T. Azuma. 2000. Reevaluation of stoichiometry and affinity/avidity in interactions between anti-hapten antibodies and mono- or multi-valent antigens. *Mol. Immunol.* 37:1111–1122. http://dx.doi.org/10.1016/S0161-5890(01)00028-1

Oishi, H., T. Tsubaki, T. Miyazaki, M. Ono, M. Nose, and S. Takahashi. 2013. A bacterial artificial chromosome transgene with polymorphic Cd72 inhibits the development of glomerulonephritis and vasculitis in MRL-Faslpr lupus mice. *J. Immunol.* 190:2129–2137. http://dx.doi.org/10.4049/jimmunol.1202196

Otipoby, K.L., K.B. Andersson, K.E. Draves, S.J. Klaus, A.G. Farr, J.D. Kerner, R.M. Perlmutter, C.L. Law, and E.A. Clark. 1996. CD22 regulates thymus-independent responses and the lifespan of B cells. *Nature.* 384:634–637. http://dx.doi.org/10.1038/384634a0

Otwinowski, Z., and W. Minor. 1997. Processing of X-ray diffraction data collected in oscillation mode. *Methods Enzymol.* 276:307–326. http://dx.doi.org/10.1016/S0076-6879(97)76066-X

Phee, H., W. Rodgers, and K.M. Coggeshall. 2001. Visualization of negative signaling in B cells by quantitative confocal microscopy. *Mol. Cell. Biol.* 21:8615–8625. http://dx.doi.org/10.1128/MCB.21.24.8615-8625.2001

Powell, L.D., R.K. Jain, K.L. Matta, S. Sabesan, and A. Varki. 1995. Characterization of sialyloligosaccharide binding by recombinant soluble and native cell-associated CD22. Evidence for a minimal structural recognition motif and the potential importance of multisite binding. *J. Biol. Chem.* 270:7523–7532. http://dx.doi.org/10.1074/jbc.270.13.7523

Qu, W.M., T. Miyazaki, M. Terada, L.M. Lu, M. Nishihara, A. Yamada, S. Mori, Y. Nakamura, H. Ogasawara, C. Yazawa, et al. 2000. Genetic dissection of vasculitis in MRL/lpr lupus mice: a novel susceptibility locus involving the CD72c allele. *Eur. J. Immunol.* 30:2027–2037. http://dx.doi.org/10.1002/1521-4141(200007)30:7<2027::AID-IMMU2027>3.0.CO;2-S

Robinson, W.H., H. Ying, M.C. Miceli, and J.R. Parnes. 1992. Extensive polymorphism in the extracellular domain of the mouse B cell differentiation antigen Lyb-2/CD72. *J. Immunol.* 149:880–886.

Santiago-Raber, M.L., I. Dunand-Sauthier, T. Wu, Q.Z. Li, S. Uematsu, S. Akira, W. Reith, C. Mohan, B.L. Kotzin, and S. Izui. 2010. Critical role of TLR7 in the acceleration of systemic lupus erythematosus in TLR9-deficient mice. *J. Autoimmun.* 34:339–348. http://dx.doi.org/10.1016/j.jaut.2009.11.001

Sato, S., A.S. Miller, M. Inaoki, C.B. Bock, P.J. Jansen, M.L. Tang, and T.F. Tedder. 1996. CD22 is both a positive and negative regulator of B lymphocyte antigen receptor signal transduction: altered signaling in CD22-deficient mice. *Immunity.* 5:551–562. http://dx.doi.org/10.1016/S1074-7613(00)80270-8

Schatz, P.J. 1993. Use of peptide libraries to map the substrate specificity of a peptide-modifying enzyme: a 13 residue consensus peptide specifies biotinylation in *Escherichia coli. Biotechnology (N. Y.).* 11:1138–1143. http://dx.doi.org/10.1038/nbt1093-1138

Sgroi, D., A. Varki, S. Braesch-Andersen, and I. Stamenkovic. 1993. CD22, a B cell-specific immunoglobulin superfamily member, is a sialic acid-binding lectin. *J. Biol. Chem.* 268:7011–7018.

Swaminathan, G.J., D.G. Myszka, P.S. Katsamba, L.E. Ohnuki, G.J. Gleich, and K.R. Acharya. 2005. Eosinophil-granule major basic protein, a C-type lectin, binds heparin. *Biochemistry.* 44:14152–14158. http://dx.doi.org/10.1021/bi051112b

Tada, N., S. Kimura, Y. Liu, B.A. Taylor, and U. Hämmerling. 1981. Ly-m19: The *Lyb-2* region of mouse chromosome 4 controls a new surface alloantigen. *Immunogenetics.* 13:539–546. http://dx.doi.org/10.1007/BF00343721

Takai, T. 2005. A novel recognition system for MHC class I molecules constituted by PIR. *Adv. Immunol.* 88:161–192. http://dx.doi.org/10.1016/S0065-2776(05)88005-8

Takai, T., A. Nakamura, and S. Endo. 2011. Role of PIR-B in autoimmune glomerulonephritis. *J. Biomed. Biotechnol.* 2011:275302. http://dx.doi.org/10.1155/2011/275302

Tan, E.M. 1989. Antinuclear antibodies: diagnostic markers for autoimmune diseases and probes for cell biology. *Adv. Immunol.* 44:93–151. http://dx.doi.org/10.1016/S0065-2776(08)60641-0

Tsubata, T. 2012. Role of inhibitory BCR co-receptors in immunity. *Infect. Disord. Drug Targets.* 12:181–190. http://dx.doi.org/10.2174/187152612800564455

Tung, J.S., F.W. Shen, V. LaRegina, and E.A. Boyse. 1986. Antigenic complexity and protein-structural polymorphism in the Lyb-2 system. *Immunogenetics.* 23:208–210. http://dx.doi.org/10.1007/BF00373822

Ujike, A., K. Takeda, A. Nakamura, S. Ebihara, K. Akiyama, and T. Takai. 2002. Impaired dendritic cell maturation and increased T_H2 responses in PIR-B$^{-/-}$ mice. *Nat. Immunol.* 3:542–548. http://dx.doi.org/10.1038/ni801

Von Hoegen, I., E. Nakayama, and J.R. Parnes. 1990. Identification of a human protein homologous to the mouse Lyb-2 B cell differentiation antigen and sequence of the corresponding cDNA. *J. Immunol.* 144:4870–4877.

Wilson, K.A., J.L. Kellie, and S.D. Wetmore. 2014. DNA-protein π-interactions in nature: abundance, structure, composition and strength of contacts between aromatic amino acids and DNA nucleobases or deoxyribose sugar. *Nucleic Acids Res.* 42:6726–6741. http://dx.doi.org/10.1093/nar/gku269

Winn, M.D., C.C. Ballard, K.D. Cowtan, E.J. Dodson, P. Emsley, P.R. Evans, R.M. Keegan, E.B. Krissinel, A.G. Leslie, A. McCoy, et al. 2011. Overview of the CCP4 suite and current developments. *Acta Crystallogr. D Biol. Crystallogr.* 67:235–242. http://dx.doi.org/10.1107/S0907444910045749

Xu, M., R. Hou, A. Sato-Hayashizaki, R. Man, C. Zhu, C. Wakabayashi, S. Hirose, T. Adachi, and T. Tsubata. 2013. *Cd72^c* is a modifier gene that regulates *Fas^{lpr}*-induced autoimmune disease. *J. Immunol.* 190:5436–5445. http://dx.doi.org/10.4049/jimmunol.1203576

Ying, H., E. Nakayama, W.H. Robinson, and J.R. Parnes. 1995. Structure of the mouse CD72 (Lyb-2) gene and its alternatively spliced transcripts. *J. Immunol.* 155:1637.

Zelensky, A.N., and J.E. Gready. 2005. The C-type lectin-like domain superfamily. *FEBS J.* 272:6179–6217. http://dx.doi.org/10.1111/j.1742-4658.2005.05031.x

2706

CD72 negatively regulates anti-Sm/RNP B cells | Akatsu et al.